

This article was downloaded by:

On: 24 January 2011

Access details: *Access Details: Free Access*

Publisher *Taylor & Francis*

Informa Ltd Registered in England and Wales Registered Number: 1072954 Registered office: Mortimer House, 37-41 Mortimer Street, London W1T 3JH, UK



Journal of Macromolecular Science, Part A

Publication details, including instructions for authors and subscription information:

<http://www.informaworld.com/smpp/title~content=t713597274>

Preparation, Characterization and Drug Release Behavior of 5-Fluorouracil Loaded Carboxylic Poly(ϵ -caprolactone) Nanoparticles

Jiashi Li^a; Yan Zhang^a; Jie Chen^a; Chaohua Wang^a; Meidong Lang^{a,b}

^a Key Laboratory for Ultrafine Materials of Ministry of Education, School of Materials Science and Engineering, East China University of Science and Technology, Shanghai, China ^b Key Laboratory of Molecular Engineering of Polymers (Fudan University), Ministry of Education, Shanghai, China

To cite this Article Li, Jiashi , Zhang, Yan , Chen, Jie , Wang, Chaohua and Lang, Meidong(2009) 'Preparation, Characterization and Drug Release Behavior of 5-Fluorouracil Loaded Carboxylic Poly(ϵ -caprolactone) Nanoparticles', *Journal of Macromolecular Science, Part A*, 46: 11, 1103 – 1113

To link to this Article: DOI: 10.1080/10601320903245565

URL: <http://dx.doi.org/10.1080/10601320903245565>

PLEASE SCROLL DOWN FOR ARTICLE

Full terms and conditions of use: <http://www.informaworld.com/terms-and-conditions-of-access.pdf>

This article may be used for research, teaching and private study purposes. Any substantial or systematic reproduction, re-distribution, re-selling, loan or sub-licensing, systematic supply or distribution in any form to anyone is expressly forbidden.

The publisher does not give any warranty express or implied or make any representation that the contents will be complete or accurate or up to date. The accuracy of any instructions, formulae and drug doses should be independently verified with primary sources. The publisher shall not be liable for any loss, actions, claims, proceedings, demand or costs or damages whatsoever or howsoever caused arising directly or indirectly in connection with or arising out of the use of this material.

Preparation, Characterization and Drug Release Behavior of 5-Fluorouracil Loaded Carboxylic Poly(ϵ -caprolactone) Nanoparticles

JIASHI LI¹, YAN ZHANG¹, JIE CHEN¹, CHAOHUA WANG¹, and MEIDONG LANG^{1,2,*}

¹Key Laboratory for Ultrafine Materials of Ministry of Education, School of Materials Science and Engineering, East China University of Science and Technology, Shanghai 200237, China

²Key Laboratory of Molecular Engineering of Polymers (Fudan University), Ministry of Education, Shanghai 200433, China

Received, May 2009, Accepted June 2009

In this paper, 5-Fluorouracil (5-FU) loaded carboxylic poly(ϵ -caprolactone) nanoparticles have been prepared by emulsification/solvent evaporation o/w method, and the drug release behaviors of 5-FU were investigated. The novel carboxylic poly (ϵ -caprolactone) (P(CL-OPD)-mal) was synthesized via conjugation of maleic anhydride to sodium borohydride (NaBH_4) reduced poly(ϵ -caprolactone-co -4- carbonyl - ϵ -caprolactone) (P(CL-OPD)), while P(CL-OPD) was synthesized in bulk by ring-opening polymerization of ϵ -caprolactone and 4-carbonyl- ϵ -caprolactone (OPD) with stannous octoate as a catalyst. Their structures were confirmed by ¹HNMR, FT-IR and GPC. Dynamic light scattering (DLS), transmission electron microscopy (TEM), zeta potential measurements were used for nanoparticle characterization. TEM and DLS showed the nanoparticles were with spherical shape and uniform size distribution (mean diameter 70~100 nm), respectively. Zeta potential analysis revealed that the nanoparticles had an increased negative surface with the increase of carboxyl group concentration. UV spectroscopy was adopted to study the entrapment and release behaviour. The maximum 5-FU loading efficiency was 14.39% with the entrapment efficiency be 42%. In vitro release studies were performed in PBS at 37°C. Results of the study showed that the release behavior can be well-controlled, and the balanced release was up to 96 h. P(CL-OPD)-mal nanoparticles would provide increased benefit in biomedical and pharmaceutical applications.

Keywords: Poly(ϵ -caprolactone), 5-FU, nanoparticle, carboxyl groups

1 Introduction

Nanoparticles (NP), with size between 10 and 1000 nm, represent a very promising drug delivery system (1–3). The special size of the NP enables them to be used for carriers across biological membranes and specific targeting (4–5). The nanoparticle administration dose could be taken up by MCF-7 cells through non-specific endocytosis (6). Moreover, it is indicated that tumor vasculature was selectively permeable to colloidal carriers with diameter up to 600 nm, which enable NP to increase drug concentration at the receptor site (7–8).

Poly(ϵ -caprolactone) as a typical kind of biodegradable polymer is permeable to many kinds of drugs and has been the major area of concern to develop con-

trolled delivery systems. Previous studies suggested that poly(ϵ -caprolactone) and poly(ϵ -caprolactone) copolymers nanoparticles could be prepared by the solvent displacement method (6, 9, 10) and would provide increased therapeutic benefits by delivering the drug in the vicinity of the estrogen receptor (ER) (6). Moreover, poly (ϵ -caprolactone) nanoparticles are in the semi-crystalline state, as a result of which, these nanoparticles can act as a good candidate delivery system for oral administration and prolong the antihypertensive effect of the drug (11).

However, the simplicity of the aliphatic polyesters presents limitations in terms of functionality and physical properties. Functional groups will be beneficial to the further chemical and biological modification of the release system. Duan (12) introduced an amino group into poly(lactic acid) by copolymerization with 4-hydroxyproline, which could improve the biocompatibility of poly(lactic acid) nanoparticles. Carboxyl functional groups are also known to promote nonspecific protein adsorption and could easily form conjugation with other biological agents (11).

*Address correspondence to: Meidong Lang, East China University of Science and Technology, 130 Meilong Road, P.O. Box 391, Shanghai 200237, P. R. China Tel/Fax: 86-21-64253916; E-mail: mdlang@ecust.edu.cn.

In order to modify poly(ϵ -caprolactone), the introduction of functional groups was investigated quite intensively in recent years, such as end-functionalized poly(ϵ -caprolactone)s (13–14), chain-substituted poly(ϵ -caprolactone)s (15, 16), and pendent-functionalized poly(ϵ -caprolactone)s (17, 18). These functionalized poly(ϵ -caprolactone)s were usually synthesized by copolymerization of ϵ -caprolactone with a functionalized monomer that contains the protected functional groups which were deprotected after copolymerization (18, 19). Michael-type addition was also employed to directly functionalize the poly(ϵ -caprolactone) backbone (20). However, the complicated synthesis route and introduced toxic agents build barriers for these functionalized poly(ϵ -caprolactone)s to be fabricated into drug loaded nanoparticles. For controlled release systems, functionalized poly(ϵ -caprolactone) NP synthesized by an easier method is highly desirable. Moreover, the surface distribution of functional groups on NP will be more advantageous for receptor site target.

As is well known, 5-FU is one of the most useful anti-cancer drugs, which is widely used alone or in combination chemotherapy regimens. However, it has a short plasma half-life *in vivo* (21, 22). To maintain the effective administration of drug, 5-FU has to be dosed continually, which could cause systemic side-effects and dose-dependent. One way to diminish these unwanted side effects and reduce the toxicity of 5-FU is to entrap it in colloidal drug carriers, such as polymeric nanoparticles, which may provide a better means of delivery in terms of controlled release rate of the drug at the receptor site.

The aim of this study was to synthesize a novel carboxylic functional poly(ϵ -caprolactone) (P(CL-OPD)-mal) and fabricate it into NP with suspend carboxyl groups which could be modified by target agents. The P(CL-OPD)-mal was synthesized by three step reactions as outlined in Scheme 1. Firstly, P(CL-OPD) was synthesized by ring-opening polymerization of ϵ -caprolactone and 4-carbonyl-

ϵ -caprolactone (OPD), which was catalyzed by stannous octoate. Consequently, the carbonyls of the random copolymer P(CL-OPD) were reduced to hydroxyls by sodium borohydride (NaBH_4). Finally, maleic anhydride was conjugated to P(CL-OPD) by hydroxyl groups to get P(CL-OPD)-mal. Then, the P(CL-OPD)-mal nanoparticles with carboxyl groups at the surface and 5-FU loaded polymeric nanoparticles were prepared by the emulsification/solvent evaporation method. The release of 5-FU in the nanoparticles could be well controlled. P(CL-OPD)-mal nanoparticles are expected to have a great potential in carriers for drug controlled released delivery.

2 Experimental

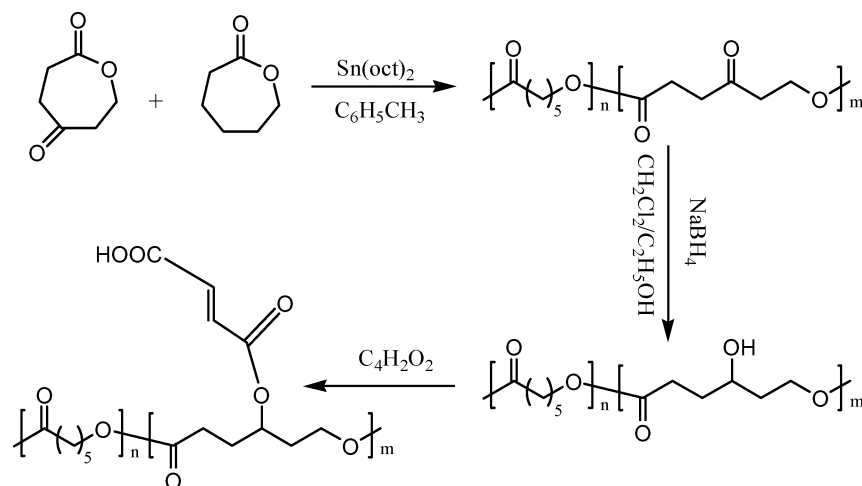
2.1 Materials

ϵ -Caprolactone (CL, Aldrich) was dried over CaH_2 for 48 h and distilled under reduced pressure at 120°C prior to use. M-Chloroperoxybenzoic acid (MCPBA, Aldrich), Stannous octoate ($\text{Sn}(\text{Oct})_2$, Aldrich), 5-fluorouracil (5-FU, kindly supplied by Zhongshan Hospital, Fudan University, China) were used as received. 2-Oxepane-1, 5-dione (OPD) was synthesized via the classical Baeyer-Villiger oxidation of 1, 4-cyclohexanedione by MCPBA as reported elsewhere (23). Toluene (Shanghai Chemical Reagent Co.) was purified by refluxing over sodium and distilled under nitrogen before use. All of the other reagents were purchased from Shanghai Chemical Reagent Co. and used without further purification.

2.2 Methods

2.2.1. Synthesis of poly(ϵ -caprolactone) with hydroxyl pendent groups

Poly(ϵ -caprolactone) with hydroxyl pendent groups was synthesized by methods previously reported (24–26).



Sch. 1. Synthetic route of P(CL-OPD)-mal

Briefly, purified OPD (0.1 mol), ϵ -CL (0.4 mol) and $\text{Sn}(\text{Oct})_2$ (0.5 mmol) were copolymerized with $\text{Sn}(\text{Oct})_2$ as a catalyst. They were stirred with 20 ml of dried toluene in an oil bath at 90°C for 24 h. Then, poly(ϵ -caprolactone-co-2-oxepane-1,5-dione) (P(CL-OPD)) was precipitated, filtered, washed with cold methanol, and dried under vacuum. Subsequently, copolymer (3 g, content of OPD groups = 5.14 mmol) and NaBH_4 (0.19 g, 5.14 mmol) were dissolved in 200 mL $\text{CH}_2\text{Cl}_2/\text{EtOH}$ (5:2, v/v) mixture under stirring for 30 min at 25°C. After CH_2Cl_2 was evaporated under reduced pressure, the rest solution was cooled to 4°C. Then the copolymer (P(CL-OPD)-OH) with hydroxyl pendent groups were recovered, filtered, washed with cold methanol, and dried under vacuum.

2.2.2. Conjugation of maleic anhydride to hydroxyl groups of P(CL-OPD)-OH

P(CL-OPD)-OH (1.599 g, Mw 17100 Da, concentration of hydroxyl groups = 2.72 mmol/g), maleic anhydride (0.2596 g) were dissolved in 50 mL CH_2Cl_2 and refluxed for 3 h at 40°C. The solvent was evaporated under reduced pressure and the residue was dropped into the petroleum ether under stirring, precipitated, filtered, washed with cold methanol, and dried under vacuum to get the product P(CL-OPD)-mal.

Acid-base Titration was used to judge the concentration of carboxyl groups of P(CL-OPD)-mal, with 0.1M NaOH as standard solution, CH_2Cl_2 as the solvent and phenolphthalein as indicator.

2.2.3. Nanoparticles preparation

NP was prepared by the emulsion/solvent evaporate technique and mini-emulsion technique. Briefly, 10 mg polymer was dissolved in 1.5 mL dichloromethane, and 10 mL of deionized distilled water of sodium dodecyl sulfate (SDS) of 0.5% (m/v) concentration, followed by ultrasonication for 80 s twice to obtain a homogeneous suspension. Then, 15 mL of deionized distilled water with SDS of 0.5% (m/v) concentration was added, and the emulsion was ultrasonicated for another 80 s twice. To prevent solvent evaporation, the above processes were all carried out in ice-water bath. The emulsion was then under magnetic stirring (600 rpm) to evaporate dichloromethane over night at room temperature. The resulting emulsion of nanoparticles was dialyzed against distilled water overnight to remove the organic solvent completely. The obtained solutions were frozen and lyophilized by a freeze-dryer system to obtain the dried nanoparticles.

2.2.4. Preparation of 5-FU loaded nanoparticles

A stock solution of 5-FU was prepared in THF. The 5-FU was encapsulated into the nanoparticles by adding a predetermined volume of 5-FU stock solution to the polymer solution. 5-FU loaded nanoparticles were prepared from the drug-polymer mixture using the method described above. The resulting emulsion was dialyzed against distilled water

for 36 h to remove the organic solvent and free 5-FU completely. The obtained solutions were frozen and lyophilized by a freeze-dryer system to obtain the dried nanoparticles.

2.3 Characterization

2.3.1. Copolymer's structure confirmation

$^1\text{H-NMR}$, FT-IR and GPC were used to characterize the structure of copolymer P (CL-OPD)-mal.

$^1\text{H-NMR}$ was performed on a Varian 500 NMR apparatus at frequencies of 500MHz, using tetramethylsilane (TMS) as internal reference in CDCl_3 . FT-IR spectra were recorded on films prepared by chloroform solution by Nicolet FT-IR spectrometer (Magna-IR 550). The copolymer molecular weights were measured by gel permeation chromatography (GPC) against polystyrene standards (Polymer Laboratories Inc.). The separation system consisted of 3 Ultrastaygel columns (2×10^5 , 1×10^5 , and 5×10^4 Å) in series. Tetrahydrofuran (THF) was the mobile phase (1.0 mL/min). Calibration curves of copolymers were obtained using standards in the 5–10 mg/mL range.

2.3.2. Morphology and size of nanoparticles

In order to observe the morphology of nanoparticles by Transmission Electron Microscope (TEM, JEM-1200-EX11), the emulsion was dropped onto copper grids directly without being dyed, then copper grids were dried in a 30°C vacuum and coated with a thin polymer film.

The particle size and the size distribution of the nanoparticles were investigated by dynamic light scattering (Autosizer 4700, Malvern) equipped with an argon laser operating at 532 nm with a fixed scattering angle of 90°. Before measurement, the nanoparticles were filtered through a 0.45 μm pore size filter to remove large aggregates.

2.3.3. Measurement of surface charge

Zeta Potential Analyzer instrument (Malvern Zetasizer 3000HS) was used to measure the surface charge of P (CL-OPD)-OH and P(CL-OPD)-mal nanoparticles. Samples were eluted by deionized distilled water to the needed concentration.

2.3.4. Drug loading content and encapsulation efficiency

The amount of 5-FU loaded in the polymeric nanoparticles was measured by UV spectroscopy. To obtain the calibration curve of 5-FU in THF, a series of solutions in the range of 1–16 $\mu\text{g}/\text{mL}$ were prepared and their absorbance at 269 nm was measured. Then the polymeric nanoparticles loaded 5-FU was also dissolved in THF, and the absorbance of the samples was interpolated in the calibration curve. The experiment was carried out in triplicate. Drug loading efficiency (DLE) and entrapment efficiency were calculated (ER) using the following equations:

$$\text{DLE} = \frac{\text{quality of drug in nanoparticles}}{\text{quality of nanoparticles}} \times 100\% \quad (1)$$

$$ER = \frac{\text{quality of drug in nanoparticles}}{\text{quality of drug added}} \times 100\% \quad (2)$$

2.3.5. *In vitro* drug release

For drug release studies, 5 mg of the freeze-dried 5-FU-loaded nanoparticles was placed in a dialysis membrane with a molecular weight cut off of 3000 g/mol. The dialysis membrane was put into 100 mL of phosphate buffer (0.1 mM; pH 7.4), placed in a shaking bath at 37°C and constant stirring rate (100 rpm). At selected time intervals, 5 mL of the phosphate buffer was withdrawn from the release medium. The volume removed from the vessel was replaced with phosphate buffer. The amount of 5-FU in the removed PBS buffer was determined by UV method described above. A series of 5-FU PBS buffer solutions in the range of 1–16 $\mu\text{g/mL}$ were prepared and their absorbance at 270 nm was measured to obtain the calibration curve of 5-FU in PBS buffer. Each sample was measured three times.

3 Results and Discussion

3.1 Synthesis and Characterization of Copolymers

In this paper, much attention has been paid to a direct functionalization for synthesizing functionalized poly (ϵ -caprolactone) which is convenient for nanoparticles fabrication. The route of synthesis of P(CL-OPD)-mal is depicted in Scheme 1. To obtain hydroxyl groups for the following conjugation, P(CL-OPD) was reduced by NaBH_4 in a solvent mixture $\text{CH}_2\text{Cl}_2/\text{EtOH}$ (5:2 vol/vol) which was reported before (20). NaBH_4 is well-known as a very mild reducing agent and could selectively reduce aldehydes and ketones rapidly at 25°C in contrast to esters. $\text{CH}_2\text{Cl}_2/\text{EtOH}$ (5:2 vol/vol) allows the reduction to be carried out

Table 1. Molecular characterization of copolymers

| Entry | F_{OPD}^a | F_{OPD}^b | M_w^c | M_n^c | PDI | F_{mal}^d |
|-----------------|----------------|-------------|---------|---------|------|----------------|
| P(CL-OPD) | 20% | 19.3% | 18800 | 12700 | 1.48 | - ^e |
| P(CL-OPD)-OH | - ^e | 19.3% | 17100 | 12100 | 1.41 | - ^e |
| P(CL-OPD)-mal-1 | - ^e | 19.3% | 8600 | 6300 | 1.36 | 0.68 |
| P(CL-OPD)-mal-3 | - ^e | 19.3% | 9600 | 5800 | 1.65 | 0.88 |

^aThe feed ratio of OPD

^bThe ratio of OPD in polymer, determined by ¹H-NMR

^cThe molecular Weight, determined by GPC

^dThe concentration of carboxyl groups, determined by Acid-base Titration, mmol/g

^eBeen not testes

under homogeneous conditions and reacting slowly enough with sodium borohydride to minimize the loss of the reducing agent. Whereas chain degradation in some scale is unavoidable because of the sensitivity of the ester units as displayed in Table 1. The molecular weight of P(CL-OPD)-OH (17100) was lower than that of P(CL-OPD) (18800) while the molecular weight distribution (PDI) was slightly decreased from 1.48 to 1.41. After all, the polyester chains are not significantly degraded by the formation of hydroxyl groups.

Maleic anhydride was subsequently conjugated to the main chain to gain a polymer with suspend carboxyl groups by esterification reaction (27). The reaction underwent easy synthesis and very mild conditions-refluxing in 50 mL CH_2Cl_2 for 3 h at 40°C. Nevertheless, due to the sensitivity of the ester units to nucleophilic attack (20), the molecular weights of P(CL-OPD)-mal present an obvious decline from the original 17100 to 8600 (P(CL-OPD)-mal-1) and 9600 (P(CL-OPD)-mal-3). Contrast of molecular weights of P(CL-OPD)-mal-1 and P(CL-OPD)-mal-3 also indicated that the amount of maleic anhydride conjugation

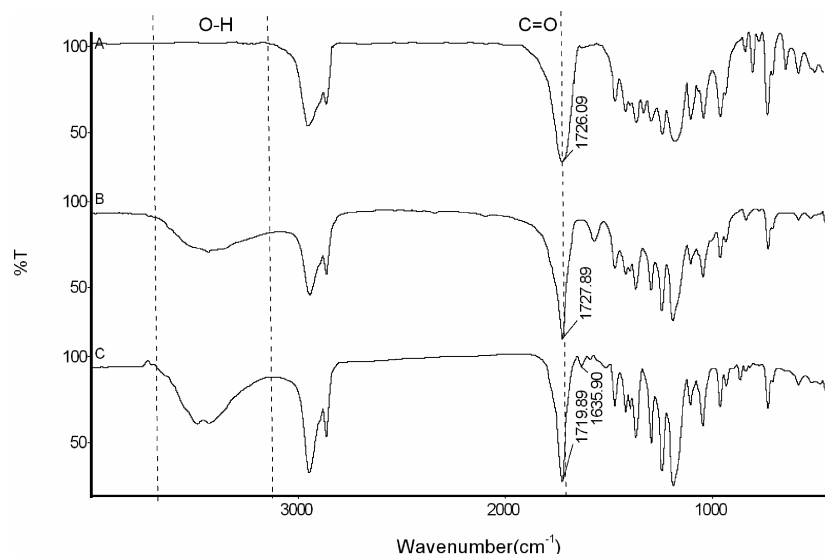


Fig. 1. FT-IR spectra of copolymers (A) P(CL-OPD), (B) P(CL-OPD)-OH, (C) P(CL-OPD)-mal.

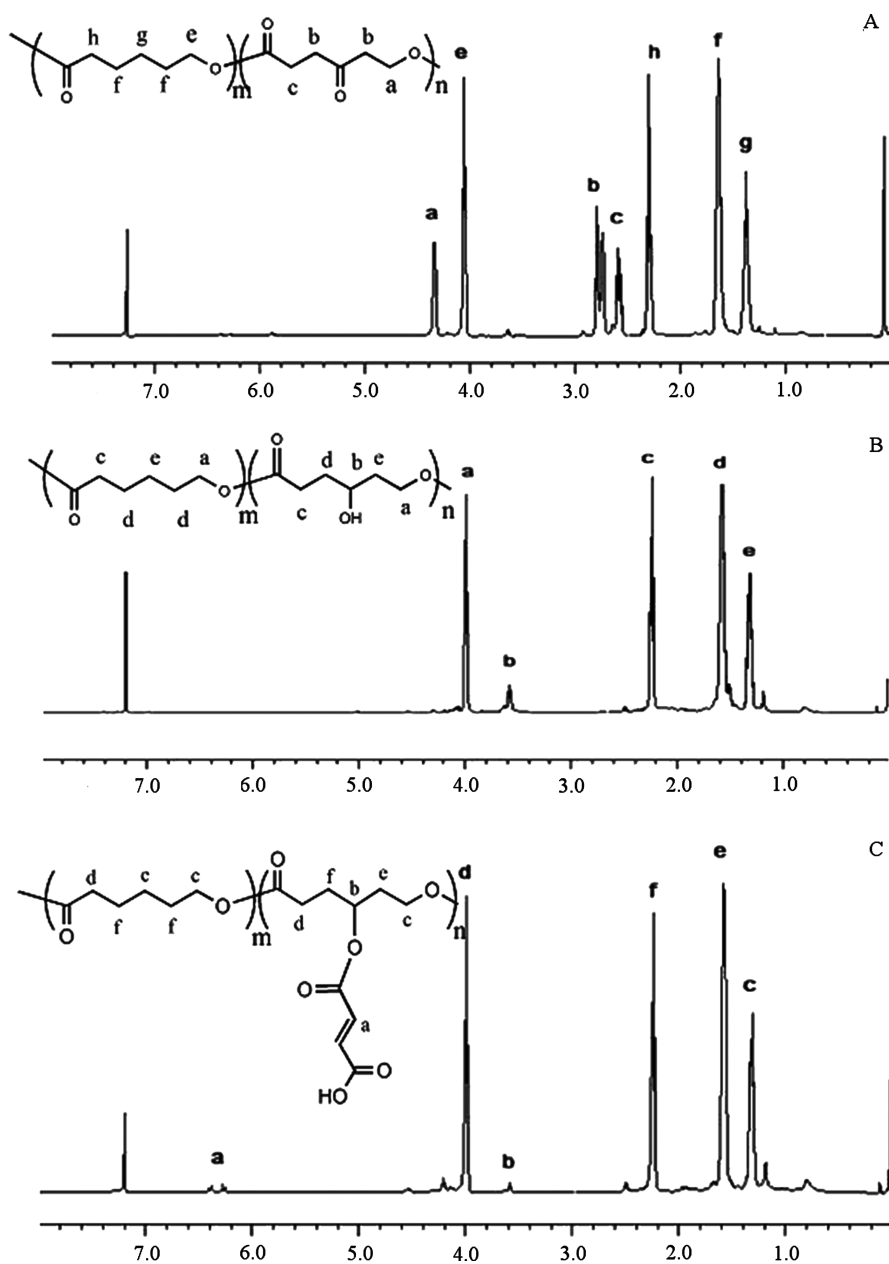


Fig. 2. $^1\text{H-NMR}$ spectra of (A) P(CL-OPD), (B) P(CL-OPD)-OH, (C) P(CL-OPD)-mal

increased with the molecular weight. Meanwhile, because of chain degradation caused by conjugation of maleic anhydride, PDI of P(CL-OPD)-mal increased with the concentration of carboxyl groups (shown in Table 1).

FT-IR spectra of copolymers P(CL-OPD), P(CL-OPD)-OH, P(CL-OPD)-mal are shown in Figure 1. An ester carbonyl stretching band of $-\text{O}-\text{C}=\text{O}$ is observed at around 1725 cm^{-1} , while a strong vibration band of $\text{C}-\text{O}-\text{C}$ appears at 1187 cm^{-1} in all the three spectrum. Comparing curve A with curve B, the ester carbonyl stretching band shifts from 1726 cm^{-1} to 1727 cm^{-1} and the intensity is weakened, which supply an evidence for the transition of carbonyl groups to hydroxyl groups. Moreover, the FI-IR spectrum

of P(CL-OPD)-OH (curve B) shows a wide vibration band of $-\text{OH}$ at around 3500 cm^{-1} . Spectrum of P(CL-OPD)-mal (curve C) shows the existence of vibration band of $\text{C}=\text{C}$ at 1635 cm^{-1} and a wide vibration band of $-\text{OH}$ at around 3500 cm^{-1} which is due to conjugation of maleic anhydride.

To further confirm the formation of the copolymers, $^1\text{H-NMR}$ spectrum of P(CL-OPD), P(CL-OPD)-OH, and P(CL-OPD)-mal are displayed in Figure 2. $^1\text{H-NMR}$ resonance signals of PCL-OPD are fully attributed, as shown in Figure 2-A. OPD content (F_{OPD}) was calculated by Equation 3 from the relative intensity (I) of the appropriate resonances in the $^1\text{H-NMR}$ spectrum of the purified products.

The comonomer conversion exceeded 95% within 48 h and F_{OPD} (valued 0.2) agreed with the composition of the feed ratio (Table 1).

Figure 2-B shows $^1\text{H-NMR}$ signals of P (CL-OPD-OH) after reduction. The peaks for $-\text{COOCH}_2-$ (H_a' in Figure 2-A) in OPD units at 4.35 ppm clearly disappear. The triplets at 2.60 ppm, 2.75 ppm, 2.80 ppm and 4.34 ppm in Figure 2-A are indeed shifted back to high fields, resulting in some overlapping with the signals of PCL protons. All of these indicate the ketone pendent groups of copolymer P(CL-OPD) are completely reduced to hydroxyl pendent groups by NaBH_4 in the $\text{CH}_2\text{Cl}_2/\text{C}_2\text{H}_5\text{OH}$ mixture.

$$F_{\text{OPD}} = \frac{I_{a'}}{I_{a'} + I_a} = \frac{I_{c'}}{I_{c'} + I_c} = \frac{I_{d'} + I_{d''}}{I_{d'} + I_{d''} + I_d} \quad (3)$$

The $^1\text{H-NMR}$ signals of P(CL-OPD)-mal are observed in Figure 2-C. As absent in Figure 2-B, the peaks for maleic anhydride unit proton $-(\text{COOC}-\text{CH}=\text{CH}-\text{COOH})$ are observed at 6.23 ppm and 6.40 ppm (H_a in Fig 2-C). It confirms the conjugation of maleic anhydride.

In the present study, the primary consideration is to synthesize poly(ϵ -caprolactone) with suspended carboxyl groups. Therefore, the content of carboxyl groups is of importance for the property of the synthesized copolymer and nanoparticles. We discussed the influence of mol feed ratio of copolymer to maleic anhydride on the concentrations of carbonyl groups. Acid-base Titration was used to judge the concentration of carboxyl groups of P(CL-OPD)-mal. Because of the steric hinderance of pendent hydroxyl groups and mild reaction conditions, the efficiency of maleic anhydride conjugation was equally low when the feed ratio of copolymer to maleic anhydride was 1:1. Increasing of the feed ratio of maleic anhydride could enhance the efficiency of maleic anhydride conjugation. As indicated in Table 2, the concentration of carboxyl groups increases from 0.68 mmol/g to 1.40 mmol/g with the feed ratio of copolymer to maleic anhydride changed from 1:1 to 1:3. When the feed ratio increased to 1:5, the content of carboxyl groups did not increase any more and may lead to side reactions. As a result, the copolymer with alterable carboxyl group concentration in some scale could be obtained.

Table 2. The influence of mol feed ratio on carbonyl groups concentrations in copolymer

| Entry | P(CL-OPD): Mal (mol/mol) | Carboxyl groups concentration (mmol/g) |
|-----------------|-----------------------------|---|
| P(CL-OPD)-mal-1 | 1:1 | 0.68 |
| P(CL-OPD)-mal-2 | 1:1.5 | 0.87 |
| P(CL-OPD)-mal-3 | 1:2 | 0.88 |
| P(CL-OPD)-mal-4 | 1:2.5 | 1.20 |
| P(CL-OPD)-mal-5 | 1:3 | 1.40 |
| P(CL-OPD)-mal-6 | 1:5 | 1.38 |

3.2 Characterization of Nanoparticles

In the previous research (9–10, 28–29), poly (ϵ -caprolactone) (PCL) microparticles or nanoparticles were prepared either by the oil-in-water (o/w) or the water-in-oil-in-water (w/o/w) solvent evaporation methods. The choice of encapsulation method usually depends on the solubility characteristics of the drug. Water-insoluble drugs with hydrophobic polymers were commonly encapsulated by the o/w emulsion solvent evaporation method which was superior to w/o/w solvent evaporation method (27). The results obtained by other investigators revealed that the microparticle diameters by the o/w-method were significant smaller than that by the w/o/w-method. Contrary, the encapsulation efficiency with the o/w-method was higher than that with the w/o/w-method (28).

In our approach, an improved o/w emulsion solvent evaporation method was adopted since 5-FU was water-insoluble. The method involved two major steps, the pre-emulsification of an organic phase containing solvent and polymer in an aqueous solution containing surfactant; the subsequent emulsification in equal aqueous solution and removal of solvent from the droplets of the emulsion. Meanwhile, miniemulsion technique was employed by using high shear. It is reported that nanoparticles distribution could be well controlled by miniemulsion technique (29). Additionally, by mini-emulsion process it is possible to form the nanodroplets from low or highly viscous polymeric solutions (10).

The particle size and nanoparticle stability have been optimized by varying the amount of surfactant and the carboxyl group content, as well as the property and volume of the internal oil phase. The prepared nanoparticles (5-FU unloaded and loaded) were characterized in terms of mean size and size distribution, morphology and surface charge. The effect of several variables on the characteristics of the NP were evaluated, just as internal oil phase and the concentration of SDS (0, 0.5, 0.1, 0.15 and 0.2 mg/mL) as well as the carboxyl group content of the copolymer (0.68, 0.88, 1.40 mmol/g).

3.2.1. Effects of the formulation variables on the nanoparticle properties

3.2.1.1. Effect of the internal oil phase on the nanoparticles.

The solvent chosen in the preparation of emulsion should satisfy three conditions: low boiling point, good volatility; be inert to the loaded drugs; equal solubility in water. Consequently, in the subsequent removal of solvent from the droplets, the solvent is easy to transfer into the water which could accelerate the solidification of the polymer domain. Therefore, we chose dichloromethane and ethyl acetoacetate as the tentative solvent.

To some extent, the stability of emulsion depends on the proportion of oil phase. Research revealed that the stability of emulsion increases with the proportion of oil phase in some scale. Meanwhile, the viscosity of oil phase increased

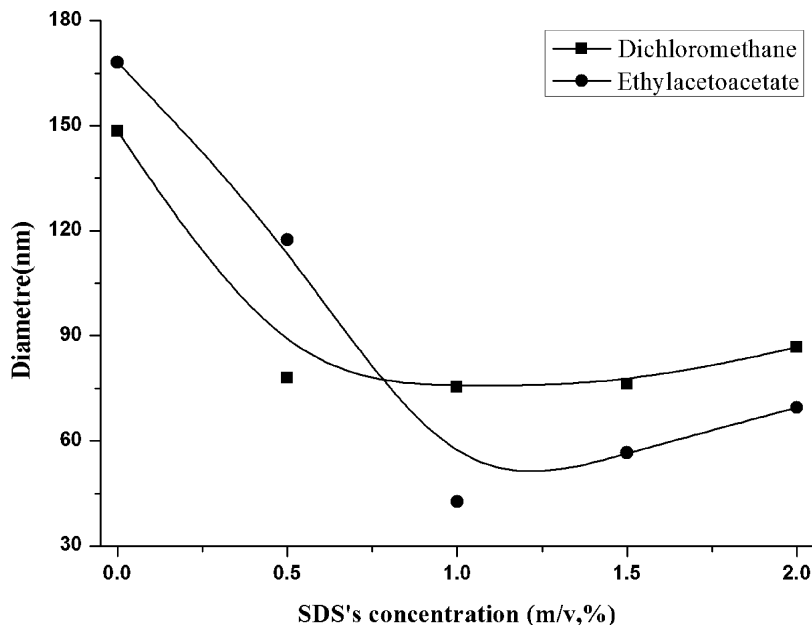


Fig. 3. The effect of SDS concentration on the particle size.

with the polymer concentration increasing, which could accelerate the solidification of the phase-separated polymer domain and leads to the increase in particle size as well as the decrease in drug loss. Take these elements into account, we dissolved 10 mg polymer into 1.5 mL solvent.

3.2.1.2. Effect of SDS on the particle size and distribution.

The type and concentration of surfactant are related to a great extent to stabilize the initial emulsion and the final solid particles at the end of the formulation process. Therefore, we studied the effect of surfactant (SDS) on the particles size and distribution. Firstly, effect of surfactant concentration on NP was discussed respectively in dichloromethane and ethyl acetoacetate to ensure the finally chosen solvent. As shown in Figure 3, when the concentration of SDS was below 1% (m/v), the particle size decreased with the increasing of SDS concentration. However, when the SDS concentration increased to 1.5% (m/v), the particle size almost stayed and even increased, which could be attributed to that the higher concentration of SDS cannot divide the oil phase into smaller domain anymore but deposited on the particles (10). A comparison of the two different solvents we chose, dichloromethane and ethyl acetoacetate, shows that the size of particles formed in dichloromethane was almost stayed when the SDS concentration was more than 0.5% (m/v) while that with ethyl acetoacetate was affected more intensely by the SDS concentration. Furthermore, boiling point of dichloromethane (39.8°C) is much lower than that of ethyl acetoacetate (77.1°C), which enables dichloromethane to evaporate faster than ethyl acetoacetate from the emulsion. Accordingly, NP formed in dichloromethane possessed a smaller size than that formed in ethyl acetoacetate when the content

of SDS was lower than 0.5% m/v. As the SDS concentration increased to 1.0% m/v, the influence of solvent solubility became dominant. NP formed in ethyl acetoacetate became smaller than that in dichloromethane (displayed in Fig. 3). Take into account the amount of SDS added and NP particle size, dichloromethane was a more suitable solvent.

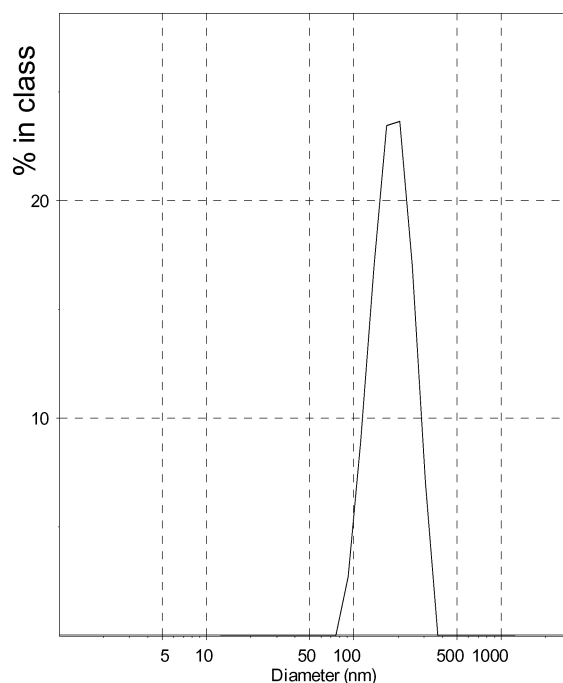


Fig. 4. Size distribution of P(CL-OPD) -mal particles without SDS.

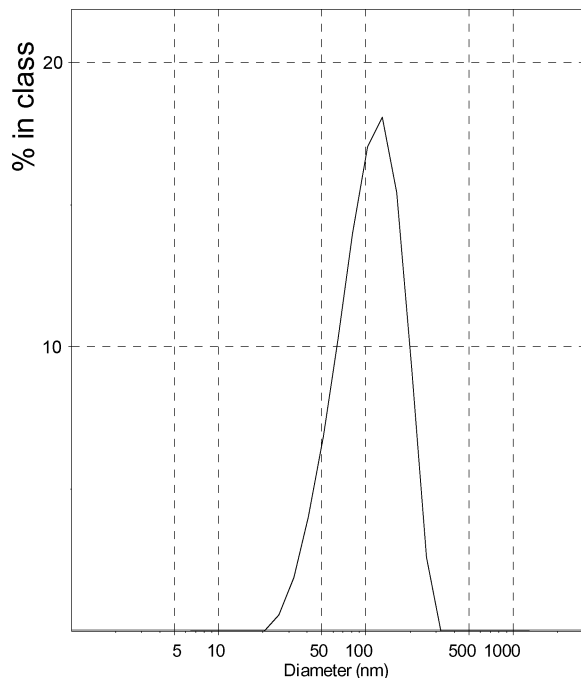


Fig. 5. Size distribution of P(CL-OPD)-mal particles with SDS.

Figure 4 and 5 display the effect of SDS on the size distribution of NP formed in dichloromethane. While the addition of SDS decreases the NP size, it enlarges the size distribution. The polymeric nanoparticles (carboxyl groups concentration = 0.68 mmol/g) without SDS have a narrower unimodal distribution (polydispersity = 0.124) than that of nanoparticles (carboxyl groups concentration

= 0.68 mmol/g) with SDS 0.5% (m/v) (polydispersity = 0.243).

3.2.1.3. Effects of carboxyl group concentration on the nanoparticle stability. Figure 6 displays the effect of carboxyl group concentration on the nanoparticle stability. Carboxyl groups tend to distribute on the surface of the nanoparticles, and build a hydrophilic surface for the particles, which enhance the nanoparticles dispersed stability. As the results show, with the content of carboxyl groups increasing, the diameters of particles decrease and size distribution became narrower. However, the addition of SDS broke this rule. As is shown in the Figure 6, with SDS 0.5% (m/v), the diameters and size distributions of particles were seldom affected by the carboxyl group concentration because SDS could also increase the hydrophilic of particles and the contribution of carboxyl groups to the hydrophilic was comparative tiny. Therefore, carboxyl group concentration seldom affects the NP size and stability with SDS.

3.2.2. Effects of initial drug concentration on drug loading

5-FU loaded nanoparticles possess a diameter around 100 nm with a monodisperse size which is shown in Figure 7. It has been reported that smaller particles tend to accumulate in tumor sites (30, 31). Less than 200 nm particles can prevent spleen filtration (32). In addition, smaller particles make intravenous injection easier, and their sterilization may be simply performed by filtration (33, 34).

The DLE and ER are also important factors to be considered. Therefore, we discussed the effects of different initial drug amounts on the DLE and ER, which are summarized

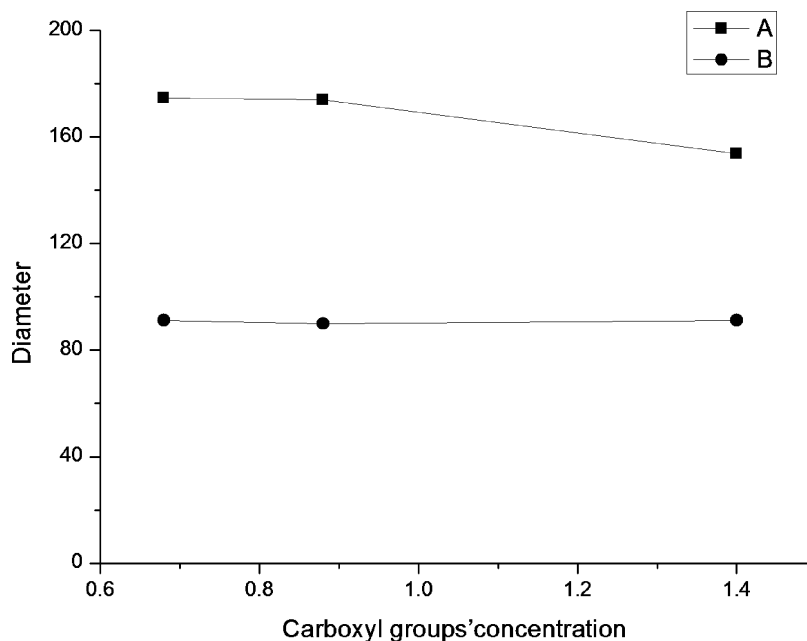


Fig. 6. The effect of carboxyl groups concentration on the nanoparticle stability (A) P(CL-OPD)-mal particles without SDS. (B) P(CL-OPD)-mal particles with SDS 0.5% m/v.

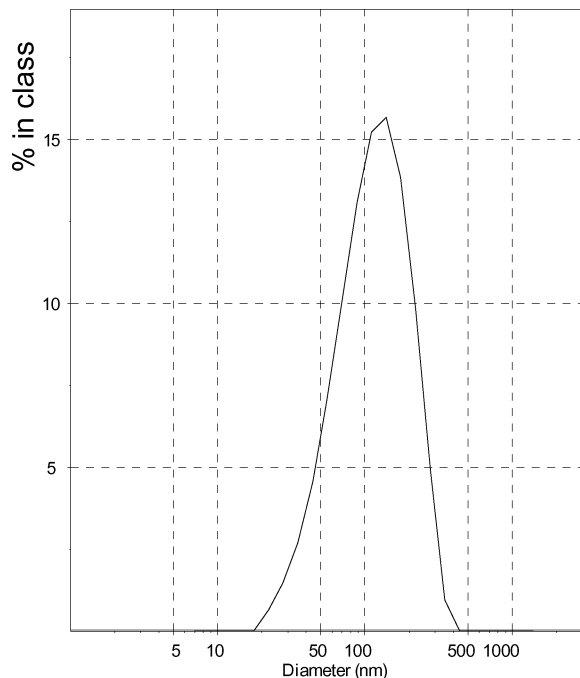


Fig. 7. Size distribution of 5-FU loaded P(CL-OPD)-mal particles.

in Table 3. With an increase in the initial drug amount from 2 to 8 mg, the ER declined drastically from 93.9 to 42.0% while DLE increased from 9.39 to 14.39%, respectively. However, the DLE of copolymer nanoparticles was still low due to the slightly water solubility of 5-FU (35).

3.2.3. Morphology

The morphology of the nanoparticles loaded 5-FU was investigated by the transmission electron microscopy (TEM) technique. Figure 8 shows the TEM image of nanoparticles. It can be shown that nanoparticles appear spherical with a monodisperse size.

3.2.4. Zeta potential analysis

P(CL-OPD)-OH NP, P(CL-OPD)-mal-2 NP, P(CL-OPD)-mal-5 NP were prepared as described above and the content of SDS in the emulsion was 0.5% m/v. Because of the localization of the SDS, all the three kinds of NP had a

Table 3. The Characteristics of 5-FU Loaded copolymer nanoparticles

| Sample | Polymer mg | SDS m/v,% | Drug mg | DLE ^a % | ER ^b % |
|--------|------------|-----------|---------|--------------------|-------------------|
| NP-A | 20 | 0.5 | 2 | 9.39 | 93.9 |
| NP-B | 20 | 0.5 | 4 | 11.28 | 63.6 |
| NP-C | 20 | 0.5 | 6 | 13.99 | 54.2 |
| NP-D | 20 | 0.5 | 8 | 14.39 | 42.0 |

^acalculated by Equation 1

^bcalculated by Equation 2

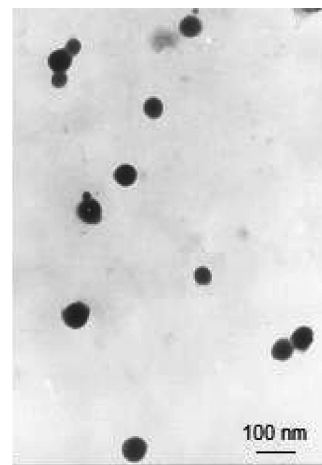


Fig. 8. TEM image of 5-FU loaded P(CL-OPD)-mal nanoparticles.

significant negative charge from -31.8 mV to -36.5 mV (P(CL-OPD)-OH \rightarrow P(CL-OPD)-mal-2. \rightarrow

P(CL-OPD)-mal-5). Meanwhile, the negative charge became stronger with the increasing of carboxyl group concentration in copolymer. With carboxyl group concentration of 0.68 mmol/g, P(CL-OPD)-mal-2 NP had a charge -32.7 ± 2.2 with carboxyl group concentration of 1.40 mmol/g P(CL-OPD)-mal-5 NP had a charge, -36.5 ± 1.5 . This indicated that the content of carboxyl groups congregated on the nanoparticles surface accorded with that in the copolymer. Hereby, the adjustment of carboxyl group concentration on the NP surface could be realized by the variety of that in the copolymer.

3.3 In Vitro Release

Figure 9 illustrates the drug release curves *in vitro* of 5-FU loaded copolymer nanoparticles. For all NP, 5-FU release occurred in two phases: (i) in the first 8 h, 5-FU had an initial burst release. The cumulative release amount was only 53% \sim 57%. It is attributed to the fraction of the drug absorbed on the large surface area of the nanoparticles instead of that incorporated in nanoparticles; (ii) after the initial burst, the nanoparticles possessed a slower, balanced release for up to 96 h, resulting from the diffusion of the drug dispersed into the polymer matrix.

To confirm the effect of polymer-drug interaction on the rate of drug release from copolymer nanoparticles, we investigated the release behavior of drug loading 11% (curve a) and 14% (curve c), and that with carboxyl groups concentration 0.68 mmol/g (P(CL-OPD)-mal-1, curve b) and 1.20 mmol/g (P(CL-OPD)-mal-4) (curve c). As shown in Figure 9, the release rate of P(CL-OPD)-mal-4 was slower than that of P(CL-OPD)-mal-1. This clearly demonstrates that the carboxyl group concentration has an effect on drug release. Especially, the initial burst release was lightened by the content of carboxyl groups in terms of comparison of

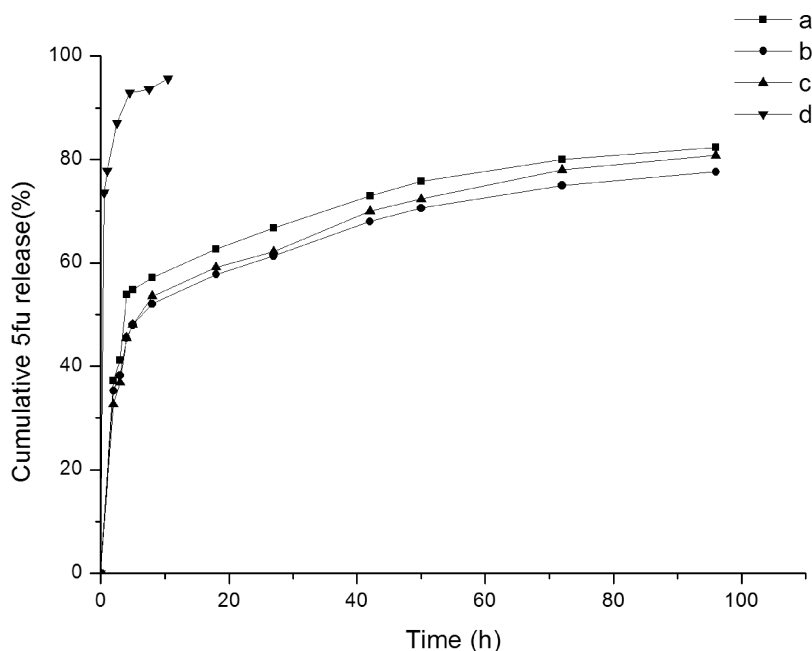


Fig. 9. Drug release curves in vitro of 5-FU loaded copolymer nanoparticles (a)P(CL-OPD)-mal-1, DLE 11%; (b)P(CL-OPD)-mal-4, DLE 11%; (c)P(CL-OPD)-mal-4, DLE 14% (d)5-FU only.

curves a and b. It is probably due to the adsorption of 5-FU on hydrophilic surface and therefore the release of 5-FU was well controlled by NP with carboxyl groups aggregation. DLE in the NP is also a parameter influencing the rate of drug release. The results showed that the cumulative release was enhanced by an increase in DLE (shown in curve b and c) as expected. Usually, a faster release rate with increasing amounts of drug in the NP is typical which can be explained by an assisted diffusion model (36).

4 Conclusions

In this study, PCL polymers bearing carboxyl side-groups were synthesized by an easy method. The polymeric nanoparticles and the 5-FU loaded nanoparticles with carboxyl groups on the surface were prepared by o/w method and miniemulsion technique. The carboxyl group concentration on the NP surface depended on that in the copolymer. Nanoparticles formulated from P(CL-OPD)-mal are about 100 nm and possess spherical structure. The particle size was influenced by the amount of surfactant and the carboxyl group content, as well as the property of the internal oil phase. The DLE and EE could be adjusted by the formulation variables. For the drug release behaviors in vitro, it has an initial burst release for the first 8 h and possesses a slower, balanced release for up to 96 h. Carboxyl group concentration and DLE have an effect on the rate of drug release. Meanwhile, the initial burst release was lightened by the content of carboxyl groups. The results show P(CL-OPD)-mal nanoparticles might have a great poten-

tial as carriers for drugs. The pendent carboxyl chain is also a good spacer for further modification. The conjugation of folic acid as the target agent to the nanoparticles is under studying, which is to be introduced in the next article.

5 Acknowledgements

This research was supported by the National Natural Science Foundation of China (20804015 and 20674019), “Shu Guang” Project of Shanghai Municipal Education Commission, Specialized Research Fund for the Doctoral Program of Higher Education (20060251015, No.200802511021) Shanghai Leading Academic Discipline Project (B502) and Natural Science Foundation of Shanghai (08ZR1406000).

References

- Schneider, G.F., Subr, V., Ulbrich, K. and Decher, G. (2009) *Nano Letters.*, 9(2), 636–642.
- Jian, Z.Y., Chang, J. Kae. and Shau, M.D. (2009) *Bioconjugate Chem.*, 20(4), 774–779.
- Miller, A.C., Bershteyn, A., Tan, W., Hammond, P.T., Cohen, R.E. and Irvine, D.J. (2009) *Biomacromolecules*, 10(4), 732–741.
- Talelli, M., Rijcken, C.J.F., Lammers, T., Seevinck, P.R., Storm, G., Nostrum, C.F. and Hennink, W.E. (2009) *Langmuir*, 25(4), 2060–2067.
- Bhirde, A.A., Patel, V., Gavard, J., Zhang, G.F., Sousa, A.A., Masedunskas, A., Leapman, R.D., Weigert, R.J., Gutkind, S. and Rusling, J.F. (2009) *ACS Nano*. 3(2), 307–316.
- Chawla, J.S. and Amiji, M.M. (2002) *Int .J. Pharm.*, 249, 127–138.

7. Dellian, M., Yuan, F., Trubetosky, V.S., Torchillin, V.P. and Jain, R.K. (2000) *Br. J. Cancer*, 82(9), 1513–1518.
8. Perrault, S.D., Walkey, C., Jennings, T., Fischer, H.C. and Chan, W.C.W. (2009) *Nano Letters*, in press.
9. Zhang, H.W., Bei, J.Z. and Wang, S.G. (2007) *J. Appl. Polym. Sci.*, 106, 3757–3767.
10. Anna, M., Julia, S.W., Volker, M., Paul, W. and Katharina, L. (2008) *Macromol. Biosci.*, 8, 127–139.
11. Sinha, V.R., Bansal, K., Kaushik, R., Kumria, R. and Trehan, A. (2004) *Int. J. Pharm.*, 278, 1–23.
12. Duan, J.F. and Zheng, Y.B. (2007) *J. Appl. Polym. Sci.*, 103, 2654–2659.
13. Yoshida, E. and Osagawa, Y. (1998) *Macromolecules*, 31(5), 1446–1453.
14. Lang, M. D., Wong, R. P. and Chu, C. C. (2002) *J. Polym. Sci. Part. Polym. Chem.*, 40, 1127–1141.
15. Sebastian, S. and Helmut, R. (2007) *J. Polym. Sci. Part. Polym. Chem.*, 45, 3659–3667.
16. Riva, R., Schmeits, S., Jérôme, C., Jérôme, R. and Lecomte, P. (2007) *Macromolecules*, 40(4), 796–803.
17. Emma, L.P., Justin, J.W. and Greg, G.Q. (2006) *Aust. J. Chem.*, 59(8), 534–538.
18. Wu, R., Al-Azemi, T.F. and Bisht, K.S. (2009) *Macromolecules*, 42(7), 2401–2410.
19. Lang, M.D. and Chu, C.C. (2001) *J. Polym. Sci. Part. Polym. Chem.*, 39, 4214–4426.
20. Rieger, J., Van, B.K., Lecomte, P., Detrembleur, C., Jérôme, R. and Jérôme, C. (2005) *Chem. Commun. (Camb)*, 274–276.
21. Parulekar, W., Marsh, R., Wong, R., Mendenhall, W., Davey, P., Zlotnicki, R., Berry, S., Rout, W. and Bjarnason, G. (2004) *Int. J. Radiat. Oncol. Biol. Phys.*, 58(5), 1487–1495.
22. Cai, T.B., Tang, X. and Nagorski, J. (2003) *Bioorg. Med. Chem.*, 11, 4971–4975.
23. Latere, J.P., Lecomte, P., Dubois, P. and Jérôme, R. (2002) *Macromolecules*, 35(21), 7857–7859.
24. Tian, D., Dubois, P., Grandfils, C. and Jérôme, R. (1997) *Macromolecules*, 30(3), 406–409.
25. Tian, D., Dubois, P., Grandfils, C. and Jérôme, R. (1997) *Macromolecules*, 30(7), 1947–1954.
26. Dai, W. F., Zhu, J. Y., Shangguan, A. Y. and Lang, M. D. (2009) *Eur. Polym. J.*, 45, 1659–1667.
27. Soma, C., Bishwabhusan, S., Iwao, T., Lisa, M.M. and Richard, A.G. (2005) *Macromolecules*, 38(1), 61–68.
28. Monica, H.P., Colette, Z., Alf, L., Nathalie, U., Alain, A., Maurice, H., Roland, B. and Philippe, M. (2000) *J. Control. Release.*, 65, 429–438.
29. Yu, G.Q., Zhang, Y., Shi, X.D., Li, Z.S. and Gan, Z.H. (2008) *J. Biomed. Mater. Res.*, 84A, 926–939.
30. Park, J.H., Maltzahn, G., Zhang, L.L., Schwartz, M.P., Ruoslahti, E., Bhatia, S.N. and Sailor, M.J. (2008) *Adv. Mater.*, 20, 1630–1635.
31. Faraji, Amir. H. and Wipf, P. (2009) *Bioorg. Med. Chem.*, 17, 2950–2962.
32. Kwon, G.S. and Kataoka, K. (1995) *Adv. Drug. Delivery. Rev.*, 16, 295–309.
33. Konan, Y.N., Gurney, R. and Allemann, E. (2002) *Int. J. Pharm.*, 233, 239–252.
34. Fu, Y.J., Shyu, S.S., Su, F.H. and Yu, P.C. (2002) *Colloids. Surf. B. Biointerfaces*. 25, 269–279.
35. Zhu, L.Z., Ma, J.W., Jia, N.Q., Zhao, Y. and Shen, H.B. (2009) *Colloids. Surf. B. Biointerfaces*, 68, 1–6.
36. Castelli, F., Conti, B., Maccarrone, D.E., Conte, U. and Puglisi, G. (1998) *Int. J. Pharm.*, 176, 85–98.